Reconfiguration of Network Hub Structure after Propofol-induced Unconsciousness

Heonsoo Lee, B.S.,* George A. Mashour, M.D., Ph.D.,† Gyu-Jeong Noh, M.D., Ph.D.,‡ Seunghwan Kim, Ph.D.,§ UnCheol Lee, Ph.D.‖

ABSTRACT

Introduction: General anesthesia induces unconsciousness along with functional changes in brain networks. Considering the essential role of hub structures for efficient information transmission, the authors hypothesized that anesthetics have an effect on the hub structure of functional brain networks.

Methods: Graph theoretical network analysis was carried out to study the network properties of 21-channel electroencephalogram data from 10 human volunteers anesthetized on two occasions. The functional brain network was defined by Phase Lag Index, a coherence measure, for three states: wakefulness, loss of consciousness induced by the anesthetic propofol, and recovery of consciousness. The hub nodes were determined by the largest centralities. The correlation between the altered hub organization and the phase relationship between electroencephalographic channels was investigated.

Results: Topology rather than connection strength of functional networks correlated with states of consciousness. The average path length, clustering coefficient, and modularity significantly increased after administration of propofol, which disrupted long-range connections. In particular, the strength of hub nodes significantly decreased. The primary hub location shifted from the parietal to frontal region, in association with propofol-induced unconsciousness. The phase lead of frontal to parietal regions in the α frequency band (8–13 Hz) observed during wakefulness reversed direction after propofol and returned during recovery.

Conclusions: Propofol reconfigures network hub structure in the brain and reverses the phase relationship between frontal and parietal regions. Changes in network topology are more closely associated with states of consciousness than connectivity and may be the primary mechanism for the observed loss of frontal to parietal feedback during general anesthesia.

What We Already Know about This Topic

- Loss of feedback connectivity in frontal–parietal brain networks is associated with anesthetic-induced unconsciousness

What This Article Tells Us That Is New

- Propofol reconfigures the brain's network hub structure
- Reconfiguration of hub structure may explain the observed loss of frontal–parietal feedback connectivity

UNDERSTANDING the connectivity patterns of functional brain networks across states of consciousness has shown promise in elucidating the mechanisms of anesthetic-induced unconsciousness. Neural correlates of anesthetic-induced unconsciousness have been studied with various neuroimaging techniques,[1–6] but there has been relatively little focus on graph theoretical approaches to network changes during general anesthesia.[2,7–10]

Graph theoretical network analysis has been widely used in the study of functional architecture in the brain.[11–13] The network properties of anatomic and functional connections can reveal the efficiency with which the brain balances functional segregation and global integration.[14] The healthy brain achieves these competing goals in an efficient

* Research Fellow, Department of Anesthesiology, University of Michigan Medical School, Ann Arbor, Michigan; Doctoral Candidate, Department of Physics, POSTECH, Pohang, Korea. † Associate Professor of Anesthesiology and Neurosurgery; Faculty, Neuroscience Graduate Program; University of Michigan Medical School. ‡ Professor, Departments of Clinical Pharmacology and Therapeutics, and Anesthesiology and Pain Medicine, Asan Medical Center, University of Ulsan College of Medicine, Seoul, Korea. § Secretary General, Asia Pacific Center for Theoretical Physics; Professor, Department of Physics, POSTECH. ‖ Research Investigator, Department of Anesthesiology, University of Michigan Medical School.

Received from the Department of Anesthesiology, University of Michigan Medical School, Ann Arbor, Michigan. Submitted for publication January 24, 2013. Accepted for publication August 2, 2013. Support was provided by the National Institutes of Health, Bethesda, Maryland, Grant 1RO1GM098578 (to Dr. Mashour) and the Original Technology Research Program for Brain Science through the National Research Foundation of Korea, Yuseong-gu, Daejeon, Korea (2010-0018847). Drs. Mashour and Lee hold a patent (pending) through the University of Michigan on directed functional connectivity as a method of assessing consciousness (Application No.: 13/804,706, Filed March 14, 2013, "System and Method to Assess Causal Signaling in the Brain during States of Consciousness"). The authors declare no competing interests. The last two authors equally contributed to this article.

Address correspondence to Dr. UnCheol Lee: Department of Anesthesiology, University of Michigan Medical School, 7433 Med Sci I, 1150 West Medical Center Drive, Ann Arbor, Michigan 48105. uclee@med.umich.edu. Information on purchasing reprints may be found at www.anesthesiology.org or on the masthead page at the beginning of this issue. ANESTHESIOLOGY's articles are made freely accessible to all readers, for personal use only, 6 months from the cover date of the issue.

 Anesthesiology 2013; 119:1347-59

way through small-world network organization, in which networks are organized on a spectrum between completely random and perfectly ordered networks. In particular, hub structure—like that of an airport system—is characteristic of small-world networks in the brain, enabling fast information transmission with economic wiring cost.[15] The abnormal brain can be biased toward random or regular network structures[16] and various disease states have been associated with impaired small-world properties.[17–20]

General anesthetics modulate network structure and connection strength in the brain, reversibly disrupting both of these optimal network elements in the unconscious state.[8] Specifically, the disruption of cortical networks is associated with anesthetic-induced unconsciousness.[21–24] However, the global small-world features appear to be maintained after administration of propofol.[10] The finding of maintained small-world properties during general anesthesia is consistent with a study of isoflurane-induced unconsciousness in rats.[9] It is as yet unclear how small-world structures are maintained despite significant changes of local functional connectivity and how global network structure influences information flow in the brain. For example, a recent mathematical model study suggested that the dense posterior parietal hub structure in the human brain plays a role as a "sink" of information flow that "attracts" information from the prefrontal cortex.[20]

In this study, we hypothesized that the anesthetic propofol disrupts network hub structures. The disruption of hubs naturally induces functional segregation and inefficient information transmission, which may be related to changes in consciousness. More specifically, information in the normal brain has been suggested to flow toward the parietal region,[25] which is part of the so-called "rich club" because of the dense distribution of hub nodes.[26] Thus, a second hypothesis was that the anesthetic-induced disruption of hub structure in the posterior parietal region impedes the dominant information flow from the frontal region.

In order to investigate the hypothesis that general anesthetics modulate hub structures and disrupt information flow, we applied graph theoretical network analysis to 21-channel electroencephalogram data recorded in waking, anesthetized, and recovery states. The network properties in different frequency bands were studied, with a focus on the anesthetic effect on the hub structures. The functional brain network was defined by Phase Lag Index (PLI), which is robust with respect to the volume conduction effect as well as the choice of reference.[27] In addition, we used directed PLI (dPLI)[25] to measure the phase lead and lag relationship between frontal and parietal regions as a surrogate of directed functional connectivity.

Materials and Methods

Experiment and Electroencephalographic Recording

After institutional review board approval (Asan Medical Center, Seoul, Korea) and written/informed consent, 10 healthy male subjects (aged: 20–28 yr) were studied with identical protocols, on 2 separate days 1 week apart, using 21-channel electroencephalography (10–20 system, Fp1, Fp2, F3, F4, F5, F6, F7, F8, Fz, C3, C4, Cz, T7, T8, P3, P4, P5, P6, P7, P8, Pz). The data have been analyzed once for our previous study[8] and were reanalyzed for the current study with distinct hypotheses and techniques. Data were sampled at 256 Hz; unipolar A2 electrode was used for reference; 16-bit analog-to-digital precision by WEEG-32® (LXE3232-RF; Laxtha Inc., Daejeon, Korea).

Three states were investigated: (1) wakefulness; (2) loss of consciousness (LOC), defined as loss of response to a verbal command after induction with 2 mg/kg intravenous propofol; and (3) return of consciousness (ROC), defined as a recovery of responsiveness to verbal command. The transition moments from wakefulness to LOC and from LOC to ROC were denoted as the LOC point and ROC point, respectively. Four-minute long electroencephalographic data epochs were extracted for each state. Because of individual differences in response to the anesthetic, the LOC state was defined as the first 2-min epoch after the LOC point and the 2-min epoch right before the ROC point, which resulted in a 4-min long epoch. For the wakefulness state and the ROC state, the continuous 4-min long epoch just before the LOC point and the 4-min long epoch just after the ROC point were taken for analysis, respectively. In order to track changing network properties over the course of the experiment, we segmented 4-min long epochs for each state into 10-s long epochs (24 small moving windows) without overlap. Four frequency bands were investigated independently after band-pass filtering: δ (0.5–4 Hz), θ (4–8 Hz), α (8–13 Hz), and β (13–25 Hz). The fourth-order Butterworth filter was applied to electroencephalographic data (forward and backward), correcting the phase shifting after band-pass filtering in MATLAB Signal Processing Toolbox (MathWorks, Natick, MA). To avoid electromyographic artifact contamination, we analyzed relatively lower-frequency range data (<25 Hz) for the network analysis. All electroencephalographic data were visually inspected, and epochs with artifact contamination were removed.

PLI

The PLI is a measure of functional connectivity and is relatively robust with respect to the choice of reference and the volume conduction problem.[27] To calculate PLI, the instantaneous phases of electroencephalogram signals were calculated by Hilbert transformation. If the instantaneous phases of one signal are always ahead of the phases of the other signal in a fixed relationship (or *vice versa*), the phases of the two signals are locked completely. However, if the phase lead and lag randomly take place over time, there is no consistent phase locking. The asymmetry of phase lead or lag reflects the degree of phase locking between two signals. To measure this phase relationship, the instantaneous phase differences $\Delta\phi_t = \phi_{i,t} - \phi_{j,t}, \quad t = 1,2,\ldots,n$ (n is the number of samples

within one epoch) between two electroencephalogram channels *i* and *j* were obtained. The PLI is defined as following:

$$\mathrm{PLI}_{ij} = \left|\left\langle \mathrm{sign}\left(\Delta\phi_t\right)\right\rangle\right|, \qquad 0 \le \mathrm{PLI}_{ij} \le 1 \tag{1}$$

Sign ($\Delta\phi_t$) function results in 1 if $\Delta\phi_t$ is greater than zero, 0 if it equals to zero, and −1 if it is less than zero. Thus, PLI quantifies the degree of phase locking with the asymmetry of instantaneous phase relationship. It has a value between 0 (no locking) and 1 (perfect locking).

Directed PLI was also introduced to capture the phase lead and lag relationship as a measure of *directed* functional connectivity.[25] dPLI is easily calculated just by leaving the signs in equation (1). To normalize dPLI within 0 and 1, a Heaviside step function (where $H(x) = 1$ if $x > 0$, $H(x) = 0.5$ if $x = 0$, and $H(x) = 0$ otherwise) is used. Therefore, dPLI for two signals *i* and *j* is defined as following:

$$\mathrm{dPLI}_{ij} = \left\langle H(\Delta\phi_t)\right\rangle \tag{2}$$

On average, as the instantaneous phases of signal *i* lead the phases of signal *j*, $0.5 < \mathrm{dPLI}_{ij} \le 1$, otherwise, if the phases of signal *i* are lagged by the phases of signal *j*, $0 \le \mathrm{dPLI}_{ij} < 0.5$. dPLI and PLI have the following relation:

$$\mathrm{PLI}_{ij} = 2\left|0.5 - \mathrm{dPLI}_{ij}\right| \tag{3}$$

In this study, we applied dPLI for directed functional connectivity and PLI for undirected functional network analysis. To remove a potential bias of the finite size effect (caused by lower-frequency power spectra in anesthesia) from dPLI, we defined the unbiased functional connection in the network with surrogate data. Twenty surrogate data sets were generated from each subject's electroencephalogram recordings. For generation of surrogate data, phases are randomly assigned after Fourier transformation for each channel, such that surrogate data have the same power spectra as that of original data.[28] For a connection pair of *i* and *j*, if the distribution of 20 dPLI values of surrogate data were deviated from dPLI of original data, the pair of *i* and *j* was deemed to be a true connection. Otherwise, it was considered to be disconnected ($\mathrm{dPLI}_{ij} = 0.5$). Nonparametric Wilcoxon signed-rank test was performed so that the median of 20 dPLI values of surrogate data were compared with the dPLI of original data. (H_0 [null hypothesis]: 20 dPLI values of surrogate data [$\mathrm{dPLI}_{ij}^{\mathrm{surrogate}}$] have symmetric distribution with median μ, where μ is the dPLI of original data [$\mathrm{dPLI}_{ij}^{\mathrm{original}}$].)

$$\mathrm{dPLI}_{ij} = \mathrm{dPLI}_{ij}^{\mathrm{original}} - \mathrm{median}\left(\mathrm{dPLI}_{ij}^{\mathrm{surrogate}}\right) + 0.5, \quad \text{if } P < 0.05$$
$$\mathrm{dPLI}_{ij} = 0.5 \text{ otherwise}$$

Next, a functional network was generated by transforming the dPLI matrix to the PLI matrix *via* equation (3). The functional network is a weighted and undirected network, in which each edge contains strength without direction. The proportions of nonzero edges among all possible connections (210 pairs for 21 channels) were 68 ± 11%, 69 ± 10%, and 68 ± 9% for wakefulness, LOC, and ROC, respectively. We tested the same network measures for fully connected weighted networks without generating surrogate data, and there were no qualitative differences in the results between the two schemes. The schematic representation of analysis is described in figure 1. All analysis was conducted with MATLAB.

Graph Analysis

Network properties are calculated based on the undirected, weighted functional network defined by PLI; see table 1 for a glossary of graph theory/network terminology. Each node in the network represents each electroencephalogram sensor and each edge represents the PLI between a pair of sensors. The average path length (L_w) is defined as the average of shortest path lengths (L_{ij}) between all pairs of nodes in a network. Here, we followed Latora and Marchiori.[29] By taking a harmonic mean in equation 4 we were able to prevent infinite average path length due to disconnected links.

$$L_w = \frac{1}{\frac{1}{N(N-1)}\sum_{ij}\frac{1}{L_{ij}}}, \qquad N = 21 \tag{4}$$

A clustering coefficient represents how given nodes in a graph tend to cluster together.[30] A clustering coefficient can be defined for each node (equation 5). w_{ij} is the weighted edge, or connection strength (=PLI_{ij}) between node *i* and *j*. We used the formula introduced by Stam *et al.*,[17] which is the modified version of that used by Onnela *et al.*[31] The clustering coefficient (C_w) for a given network was obtained by averaging all clustering coefficients of individual nodes (C_i) (see equations 5 and 6). A high value of clustering coefficient implies a network with highly clustered or regular structure.

$$C_i = \frac{\sum_{j\neq i}\sum_{\substack{k\neq i\\ k\neq j}} w_{ij}w_{jk}w_{ki}}{\sum_{j\neq i}\sum_{\substack{k\neq i\\ k\neq j}} w_{ij}w_{ki}} \tag{5}$$

$$C_w = \frac{1}{N}\sum_{i=1}^{N} C_i \tag{6}$$

where *j* and *k* run for neighboring nodes of node *i*, and *N* is the total number of nodes (=21).

To explore the modular structure of functional brain networks, we measured modularity[32,33] defined by equation 7. A network with high modularity has strong connections *within* modules and weak connections *between* modules. Here A_{ij} is the adjacency matrix (PLI matrix) and *m* is the total sum of connection strengths in a network. $A_{ij} - P_{ij}$ implies an actual minus expected connection strength between nodes *i* and *j* in a null model. That is, connection strength (PLI_{ij}) of the original network is compared with that of a randomized model network in which edges are randomly distributed, preserving

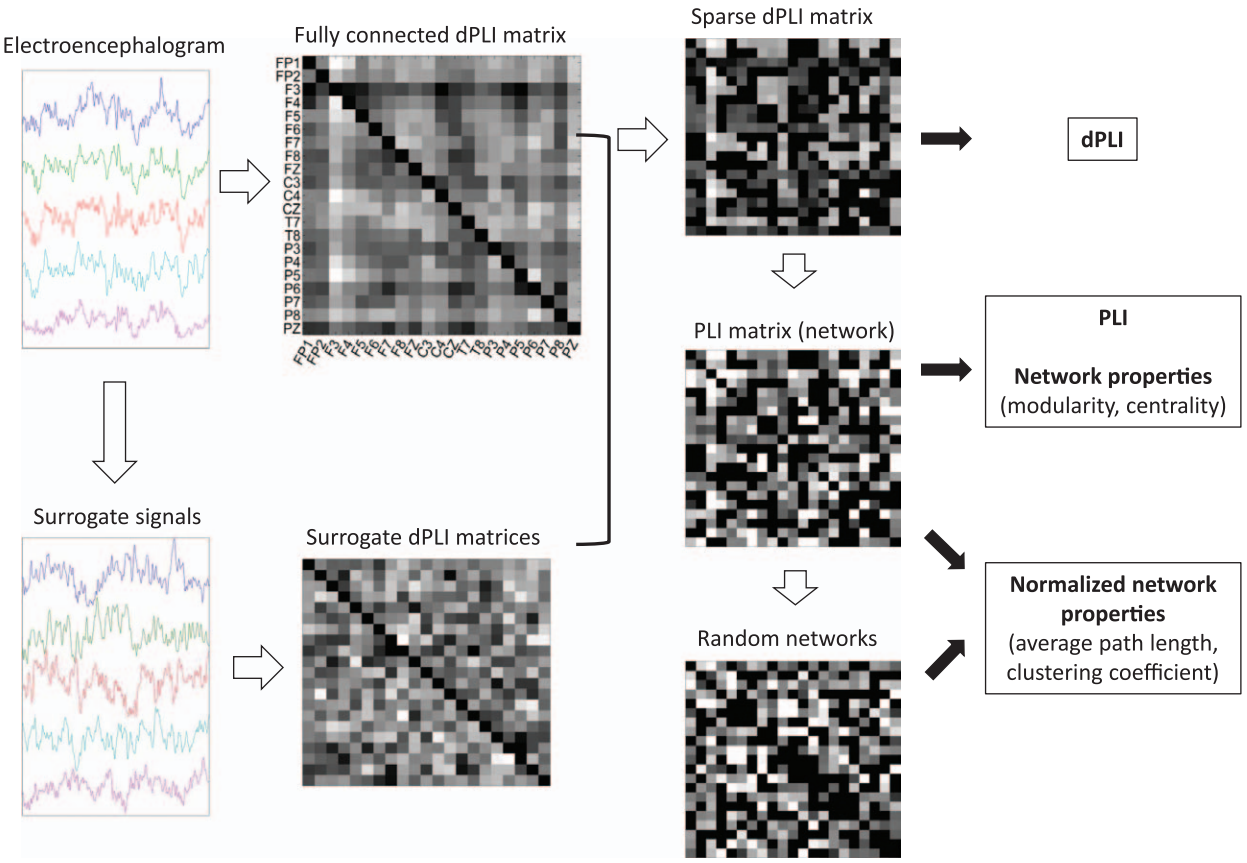

Fig. 1. Schematic representation of analysis. For each original and surrogate data set, directed Phase Lag Index (dPLI) matrices were generated (only five signals are shown). The fully connected dPLI matrix becomes sparse *via* the Wilcoxon signed-rank test. The diagonal and disconnected components are denoted in *black* whereas others are denoted in *gray*. This dPLI matrix is transformed to Phase Lag Index (PLI) matrix, resulting in an undirected weighted network. Some network properties (average path length, clustering coefficient) are measured with normalization of a random network whereas others (modularity and centrality) are measured only with the PLI network.

the degree of each node in the original network. Details of the null model and determination of expected connection strength (P_{ij}) are well described in the study by Newman.[33] c_i denotes module index of node i so that δ (c_i, c_j) assigns 1 if nodes i and j belong to the same module ($c_i = c_j$) and 0 otherwise ($c_i \neq c_j$). In summary, modularity measures the sum of connection strengths within modules after eliminating the null model effect. Finally, modularity is obtained by finding optimal combination c_i maximizing Q.

$$Q = \frac{1}{2m}\sum_{ij}\left[A_{ij} - P_{ij}\right]\delta\left(c_i, c_j\right) \quad (7)$$

We followed the Louvain algorithm[34] and used a brain connectivity tool box[35] for computing modularity (Q). Due to its heuristics in the algorithm, Q was computed 10 times per each network and the average value was taken.

In current study, we hypothesized that anesthetics disrupt the hub structure of functional brain networks, as reflected by altered centrality measures. Two popular centrality measures, betweenness and degree centrality, were used. For a given node, the betweenness centrality is defined by counting the number of shortest paths that pass through that node. Because path length varies inversely with efficiency, a node that more frequently facilitates shorter path lengths contributes to greater network efficiency. The degree centrality is defined by the total connection strengths of edges connected to a node. The relative degree centrality is defined as the proportion of the degree centrality of a node over the total sum of degree centrality of nodes. Instead, the conventional degree centrality is the absolute degree centrality. The top-ranked node in the centrality measures (betweenness and degree centrality) was determined to be a hub node. To study the correlation of the hub node and the brain region, we divided the 21 electroencephalogram channels into four brain regions: frontal, central, temporal, and parietal.

For the normalization of C_w and L_w, random networks were generated from each network and compared with original values (the average path length and clustering coefficient of a random network are denoted by L_r, C_r, respectively). Twenty random networks were generated by shuffling their edges while preserving the degree distributions.[36] C_w and L_w were divided by correlate values of the random networks. The small worldness (σ) is given by

Table 1. Description of Network Properties

Network Property	Description
Phase Lag Index	A measure for coherence based on phase relationships. This measure is robust with respect to volume conduction by ignoring zero-phase lag between brain activities.
Directed Phase Lag Index	A measure for phase lead–lag relationship between two brain activities. A consistent phase lead or lag is posited to reflect information flow between two brain activities.
Average path length	A measure for *global* efficiency of information transmission in a brain network. It quantifies the average distance of shortcuts over all pairs of nodes. The shorter the path length, the faster the information transmission in the brain.
Clustering coefficient	A measure for *local* functional segregation of brain activities. If a node has a large clustering coefficient, it indicates its neighbors are highly interconnected with each other.
Modularity	A measure for *global* functional segregation of the brain activities. The brain network can be divided into modules such that intramodular connections are maximized whereas intermodular connections are minimized. Increasing intramodular connections and decreasing intermodular connections results in higher modularity of the brain network.
Betweenness centrality	A measure for the number of shortcuts that pass through a given node. A node that enables many shortcuts may play an important role in global information transmission in the brain.
Degree centrality	A measure of the sum of connection strengths (in this study, Phase Lag Index) that are linked to a given node. A node with large number of connections may play an important role in information transmission in the brain.
Hub	In this study, a node that has a large betweenness centrality or large degree centrality is defined as a hub node. Hub structure plays a pivotal role in the coordination of information flow in the brain.
Small worldness	A measure of the balance between global integration (path length) and local segregation (clustering coefficient). Diseased brains can lose the balance between global and local organization of information.

ratio between C_w/C_r and L_w/L_r. A network is assumed to have small-world organization if σ is greater than 1 along with L_w/L_r is approximately 1.

Cortical network properties are rapidly altered after induction of anesthesia with propofol.[21] The time resolution of network changes provides important information regarding state transitions during general anesthesia. In order to visualize the time course of network properties, we segmented the electroencephalographic data into smaller windows (10-s long). To perform statistical tests, the network properties of all windows were averaged, with the mean value used to represent the network property for a subject. In other words, network properties computed from small windows were averaged to represent each state (wakefulness, LOC, and ROC) and statistically evaluated to compare these properties across three states.

Statistical Analysis

The connectivity (PLI and dPLI) and the network properties were compared across three states (wakefulness, LOC, and ROC). One-way repeated measures ANOVA was applied, with Tukey multiple comparison for each network property and each frequency band. Adjusted P value with less than 0.05 was considered to be a statistically significant difference (for the figures, $^*P < 0.05$, $^{**}P < 0.01$, and $^{***}P < 0.001$); the Geisser–Greenhouse correction was applied. Because the PLI and dPLI values were not normally distributed, nonparametric Friedman test with Dunn multiple comparisons test was performed. Regarding the two trial data sets, we assumed that the network properties and anesthetic effects across two trials were different at the 1-week interval even if the two electroencephalogram recordings were from the same subject. Thus we consider the two data sets of 10 subjects as independent from one another. GraphPad Prism Version 6.01 (GraphPad Software Inc., San Diego, CA) was used for these statistical tests.

Results

Connectivity Measured by PLI Does Not Vary with State of Consciousness

Figure 2 demonstrates that propofol induces various changes of functional connectivity, as measured by PLI. The PLIs for the four frequency bands significantly increased or decreased across states, but were not correlated with the state transitions (0.5–4 Hz: $P < 0.001$, 4–8 Hz: $P = 0.058$, 8–13 Hz: $P = 0.002$, 13–25 Hz: $P = 0.058$). The PLI of 0.5–4 Hz increased after propofol (wakefulness *vs.* LOC: $P < 0.001$) and maintained high values during the ROC (wakefulness *vs.* ROC: $P < 0.01$). In contrast, no significant changes were found in 4–8 Hz, 8–13 Hz, and 13–25 Hz frequency bands between wakefulness and the LOC ($P > 0.05$). Despite other significant changes, the PLI itself does not appear to correlate with the state of consciousness.

Network Structure Varies with State of Consciousness

In contrast to the connection strength (based on PLI), the topological properties of the network correlated well with state of consciousness (fig. 3). For the four frequency bands, L_w/L_r significantly increases after propofol induction, losing efficient global information transmission capacity (0.5–4

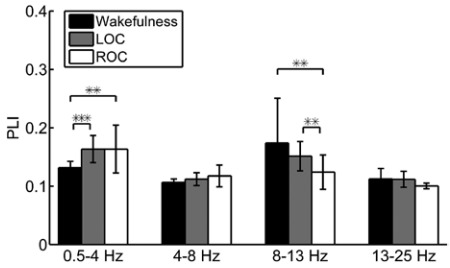

Fig. 2. Different frequency bands show different functional connectivity during general anesthesia. The Phase Lag Index (PLI) averaged over all windows and subjects for 0.5–4 Hz increases whereas the PLIs of other frequency ranges do not show significant changes after loss of consciousness (LOC). The changed PLI after anesthesia does not return to its original values after recovery of consciousness (ROC). The *error bar* indicates SD (***P* < 0.01 and ****P* < 0.001; adjusted *P* values after Dunn multicomparison tests).

Hz: $F(2,19) = 37.04$, $P < 0.001$; 4–8 Hz: $F(2,19) = 19.18$, $P < 0.001$; 8–13 Hz: $F(2,19) = 31.86$, $P < 0.001$; 13–25 Hz: $F(2,19) = 108.4$, $P < 0.001$) (wakefulness *vs.* LOC: $P < 0.001$ for all frequency bands), and recovers in association with ROC (LOC *vs.* ROC: $P < 0.001$ for all frequency bands; fig. 3A). After the induction, C_w/C_r also increases reflecting increased local functional segregation (0.5–4 Hz: $F(2,19) = 1.231$, $P = 0.303$; 4–8 Hz: $F(2,19) = 4.603$, $P = 0.016$; 8–13 Hz: $F(2,19) = 8.888$, $P < 0.001$; 13–25 Hz: $F(2,19) = 9.542$, $P < 0.001$; fig. 3B). The increased C_w/C_r for α frequency bands (8–13 Hz) did not return to the original levels after ROC (wakefulness *vs.* LOC: $P < 0.01$ for 8–13 Hz; LOC *vs.* ROC: $P < 0.01$ for 4–8 Hz). In figure 3C, Q shows a similar changing pattern with C_w/C_r across states (0.5–4 Hz: $F(2,19) = 3.959$, $P = 0.027$; 4–8 Hz: $F(2,19) = 3.743$, $P = 0.033$; 8–13 Hz: $F(2,19) = 8.113$, $P = 0.001$; 13–25 Hz: $F(2,19) = 62.95$, $P < 0.001$) (wakefulness *vs.* LOC: $P < 0.001$ for 13–25 Hz). Figure 3D shows that all networks across the three states have small worldness (σ >1 with L_w/L_r approximately 1). Interestingly, the small worldness (σ) is not changed after anesthesia (0.5–4 Hz: $F(2,19) = 2.691$, $P = 0.081$; 4–8 Hz: $F(2,19) = 0.807$, $P = 0.454$; 8–13 Hz: $F(2,19) = 3.31$, $P = 0.048$; 13–25 Hz: $F(2,19) = 3.741$, $P = 0.033$), but in the 13–25 Hz band it increases after ROC (LOC *vs.* ROC: $P < 0.01$ for 13–25 Hz).

In summary, we found that connection strength does not correlate well with states of consciousness, whereas the topological properties reflect the state transitions. The change of topological properties indicates that propofol disrupts efficient network structures in the brain.

Hub Structure Is Reconfigured after Propofol-induced Unconsciousness

Considering the important contribution of hub structure to global network functions, the effect of propofol on the hub nodes was investigated. Figure 4 represents the average betweenness centrality of nodes (electroencephalogram channels) sorted by its rank for each state and each frequency band.

At baseline, the node in the first rank and the other nodes demonstrated a large difference in the betweenness centrality. The node in the first rank had about 50% of the possible shortest paths of the network (of 210 possible shortest

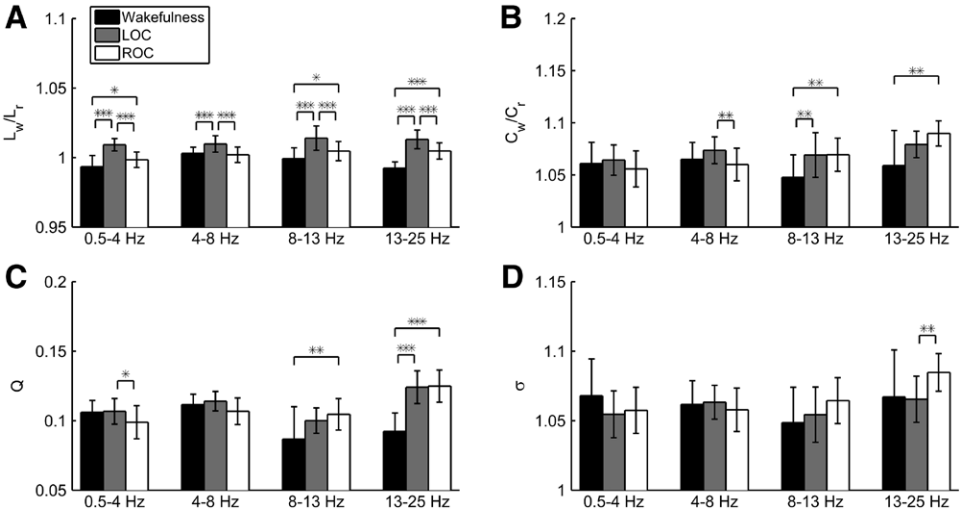

Fig. 3. Functional brain networks become segregated after loss of consciousness (LOC) and reintegrated after recovery of consciousness (ROC). (*A*) Average path length is compared after normalization by average path length of random network. The normalized average path length (L_w/L_r) increases after LOC in all frequency bands and decreases after ROC. The *error bar* indicates SD (**P* < 0.05, ***P* < 0.01, and ****P* < 0.001; adjusted *P* values after Tukey multicomparison tests). (*B*) Clustering coefficient is compared after normalization by clustering coefficient of a random network. In 8–13 Hz, the normalized clustering coefficient (C_w/C_r) increases after LOC. Recovery of C_w/C_r with ROC is shown in 4–8 Hz. (*C*) Functional brain networks become modularized after anesthesia. In 13–25 Hz, modularity (Q) increases during the LOC. (*D*) Small worldness (σ) is larger than 1 in all states and is increased after the ROC point in 13–25 Hz.

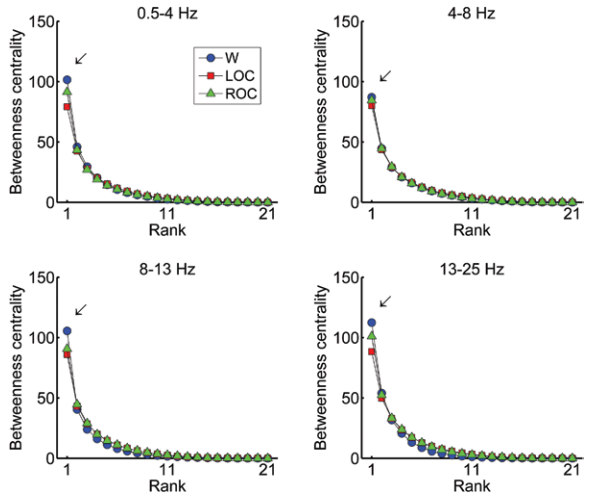

Fig. 4. Propofol affects hub nodes with the highest centrality in the brain network. The nodes are ranked in descending order of average betweenness centrality for the four frequency bands in wakefulness (W), loss of consciousness (LOC), and recovery consciousness (ROC), respectively. The highest-ranked node (defined as a hub) is mainly affected by propofol and returns with the ROC. This feature is observed in all four frequency bands.

paths). We deemed the top-ranked node as a hub in the network for each state. After LOC, the hub nodes in the networks for all frequency bands lost their strong centrality, whereas the nodes in lower ranks tended to gain centrality. In other words, in the LOC period, the capacity of the top-ranked node (hub) becomes redistributed to the other nodes.

Figure 5A demonstrates the correlation of the betweenness centrality of the hub nodes with the state change. The betweenness centrality of the hubs is significantly reduced after LOC in all frequency bands (0.5–4 Hz: $F(2,19) = 8.865$, $P < 0.001$; 4–8 Hz: $F(2,19) = 3.143$, $P = 0.055$; 8–13 Hz: $F(2,19) = 5.414$, $P = 0.009$; 13–25 Hz: $F(2,19) = 24.37$, $P < 0.001$) (wakefulness *vs.* LOC: $P < 0.001$ for 13–25 Hz; $P < 0.01$ for 0.5–4 Hz; $P < 0.05$ for 4–8 and 8–13 Hz) and tends to recover after the ROC point. Statistical significance of recovery was found in the β band (LOC *vs.* ROC: $P < 0.001$ for 0.5–4 and 13–25 Hz). Figure 5B shows the proportions (%) of four brain regions (frontal, central, temporal, and parietal areas) to which the hub nodes belong. The locations of the hub nodes from 480 networks (10 subjects × 2 experiments × 24 windows) were investigated for each state and frequency band. The proportion of parietal hubs diminishes after LOC, whereas the proportion of frontal hubs increases after LOC, especially for α (8–13 Hz) and β (13–25 Hz) bands. Regarding the state dependency, the frontal hubs are dominant after the LOC point, whereas the parietal hubs are dominant in the waking state and after the ROC point.

Figure 6 demonstrates the absolute (A) and relative (B) degree centrality for the hub nodes. The absolute degree centrality of hubs (fig. 6A) shows a similar pattern with the average connection strength measured by PLI over the frequency bands (0.5–4 Hz: $F(2,19) = 4.668$, $P = 0.015$; 4–8 Hz: $F(2,19) = 3.008$, $P = 0.061$; 8–13 Hz: $F(2,19) = 7.770$, $P = 0.002$; 13–25 Hz: $F(2,19) = 10.57$, $P < 0.001$). However, the relative degree centrality of hubs correlates well with the state change, which is similar to the betweenness centrality (a topological property; fig. 6B). The relative degree centrality suggests a diminished hub structure after LOC (0.5–4 Hz: $F(2,19) = 9.559$, $P < 0.001$; 4–8 Hz: $F(2,19) = 6.264$, $P = 0.005$; 8–13 Hz: $F(2,19) = 5.768$, $P = 0.007$; 13–25 Hz: $F(2,19) = 14.61$, $P < 0.001$) (wakefulness *vs.* LOC: $P < 0.001$ for 4–8 and 13–25 Hz; $P < 0.01$ for 0.5–4 Hz; $P < 0.05$ for 8–13 Hz), and recovery to the original level with ROC (LOC *vs.* ROC: $P < 0.01$ for 0.5–4 and 8–13 Hz; $P < 0.001$ for 13–25 Hz). Together with the result of

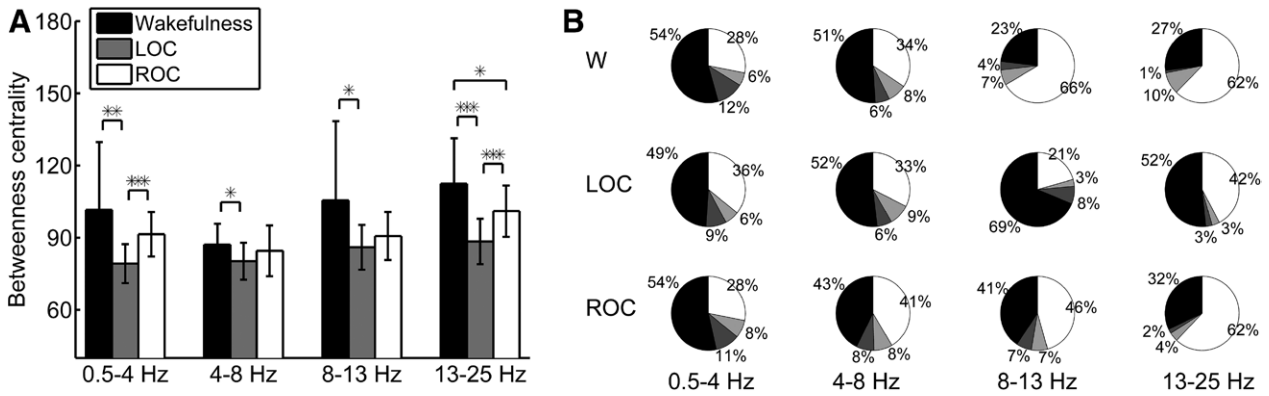

Fig. 5. The betweenness centrality of the hubs is reduced after loss of consciousness (LOC) and returns with the recovery of consciousness (ROC). (*A*) The betweenness centrality of the hub nodes is more salient in wakefulness and after ROC compared with LOC. The betweenness centrality of the hubs correlates well with the states. The *error bar* indicates SD (*$P < 0.05$, **$P < 0.01$, and ***$P < 0.001$; adjusted *P* values after Tukey multicomparison tests). (*B*) The regional proportion for the hubs of different brain regions (from *dark to light color*: frontal, central, temporal, and parietal cortices). Dominant parietal hubs (in *white*) are observed during wakefulness (W) and ROC, especially in 8–13 and 13–25 Hz. These dominant parietal hubs are diminished after LOC. Instead, the frontal region (in *black*) emerges as the dominant hub.

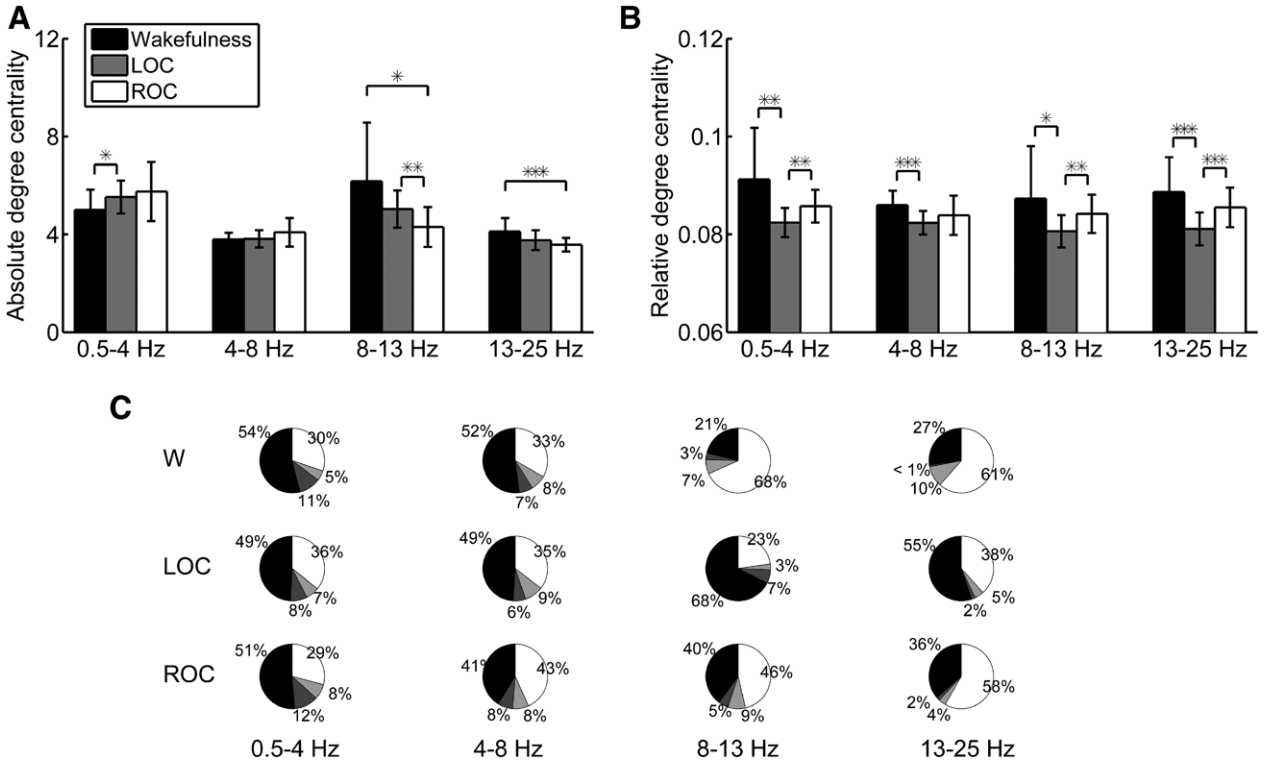

Fig. 6. The relative degree centrality of the hubs is reduced after loss of consciousness (LOC) and returns after the recovery of consciousness (ROC). (*A*) The absolute degree centrality for the hubs is variable depending on the frequency bands. The strengths were similar with those of connectivity measured by Phase Lag Index (fig. 2). The *error bar* is SD (**P* < 0.05, ***P* < 0.01, and ****P* < 0.001; adjusted *P* values after Tukey multicomparison tests). (*B*) The relative degree centrality for the hubs is reduced after LOC over all frequency bands. During the ROC, return of relative degree centrality is shown in most frequency bands. The relative degree centrality correlates with the state change. (*C*) The regional proportion for the hubs defined by highest-ranked nodes in relative degree centrality of different brain regions (from *dark to light color*: frontal, central, temporal, and parietal cortices). The parietal hubs (in *white*) are dominant during wakefulness (W), diminished after LOC, and return to dominance after ROC. The frontal region (in *black*) emerges as the dominant hub during LOC, especially over the 8–13 and 13–25 Hz bands.

betweenness centrality, the relative degree centrality reflects the topological property of a network, whereas the absolute degree centrality reflects the connection strength of a network.

Figure 6C demonstrates the same parietal hub dominance in waking and ROC states, with the frontal hub dominating in the LOC state, especially for the α (8–13 Hz) and the β (13–25 Hz) frequency bands. Both centrality measures for the hub nodes consistently suggest the diminished role of the hubs after the LOC point, especially in the parietal region.

The Phase Lead–Lag Relationship between Frontal and Parietal Regions Is Reversed after LOC

Because the hub structure plays an important role as an attractor of information flow,[25] we predicted that the disruption of parietal hubs would reverse information flow in the frontal–parietal network. In this analysis, we tested whether or not the disruption of parietal hubs after LOC point could account for the observed selective suppression of feedback connectivity, as has been found by the past studies of general anesthesia[22,37] and the vegetative state.[38] The frontal and parietal channels (9 and 7, respectively) were used for measuring the feedback and feedforward connectivity based on dPLI (fig. 7, A and B). By definition, if dPLI is larger than 0.5, the frontal phases lead the parietal phases, reflecting a dominant feedback (frontal to parietal) connectivity. Conversely, if dPLI is less than 0.5, it reflects dominant feedforward (parietal to frontal) connectivity. The average dPLI over 63 pairs of electroencephalogram channels are presented in figure 7, A and B. Because there is a possibility that dPLI can reverse phase lead–lag relationships for faster frequency bands (>13 Hz), we excluded the β frequency (13–25 Hz).[25] The feedback and feedforward connections and their temporal patterns during the experimental period are distinct over the frequency bands. In particular, the anesthetic effect is prominent in the α frequency band of 8–13 Hz (0.5–4 Hz: $P = 0.116$; 4–8 Hz: $P = 0.047$; 8–13 Hz: $P < 0.001$; fig. 7, A and B) (wakefulness *vs.* LOC: $P < 0.001$, LOC *vs.* ROC: $P < 0.01$). The feedback-dominant connectivity for α during wakefulness is disrupted after anesthesia, but soon returns to the original state after ROC point (fig. 7B; 8–13 Hz). The significant feedback-dominant connectivity (from frontal to parietal) in

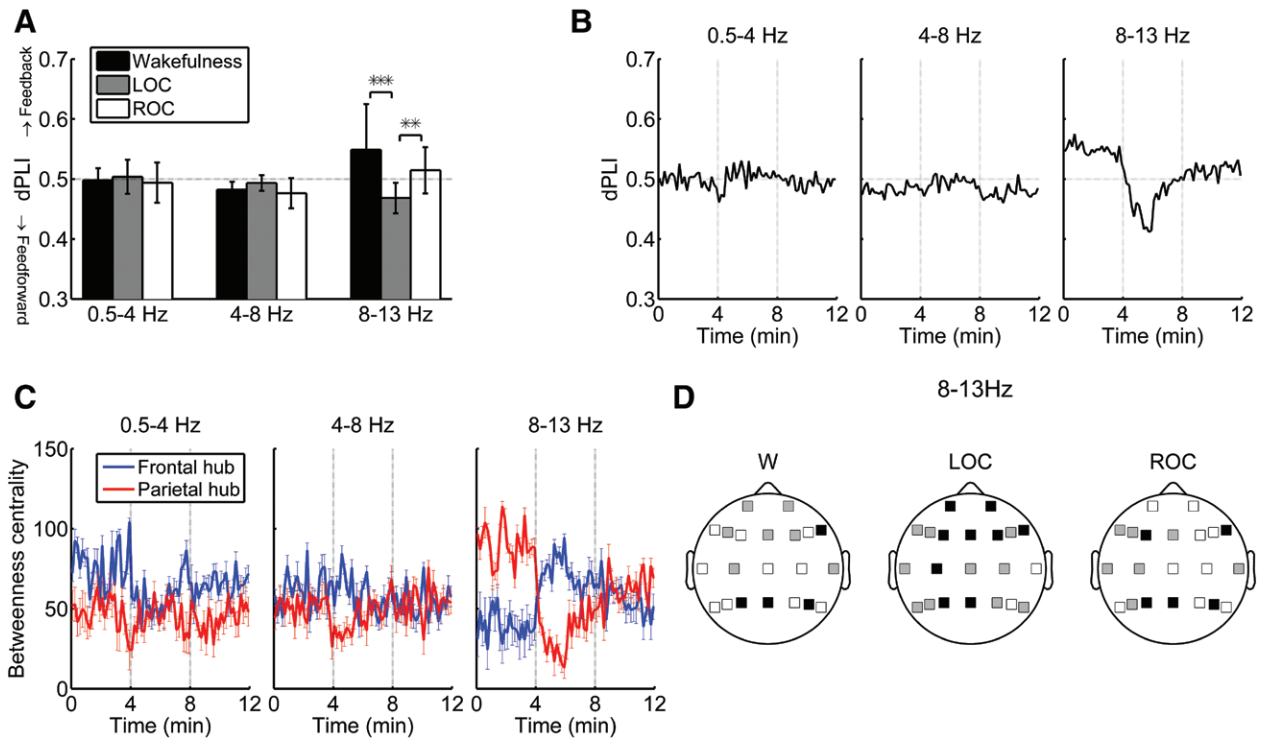

Fig. 7. Feedback-dominant connectivity is reduced in the α frequency band after loss of consciousness (LOC) and returns with recovery of consciousness (ROC). (*A*) The directed Phase Lag Index (dPLI) changes of frontoparietal connections across the three states are distinctive over the three frequency bands. The α frequency band (8–13 Hz) showed the most prominent changes according to the state transition. The *error bar* indicates SD (** $P < 0.01$ and *** $P < 0.001$; adjusted P values after Dunn multicomparison tests). (*B*) Time courses of the dPLI for three frequency bands. The time course of the α frequency band (8–13 Hz) shows the most significant change during anesthesia. (*C*) The changes of betweenness centrality of frontal and parietal hubs for the three frequency bands. The nodes with the largest betweenness centrality are selected as the hub nodes in the frontal and parietal regions. The α frequency band (8–13 Hz) manifests a significant reversal in terms of frontal and parietal hub structures. The parietal hub is dominant during wakefulness, whereas the frontal hub is dominant after LOC. This shift correlates with shifts in reversal of directional connectivity. The *error bar* indicates standard error. (*D*) The phase relationships among electroencephalogram channels in the α frequency band. The phase lead and lag relationship measured by dPLI is presented with different colors. A channel lagging in phase against the other channels is denoted by *black*. Otherwise, a channel leading in phase against the other channels is denoted by *gray*. If a channel has no significant phase lead or lag relationship (Wilcoxon signed-rank test with median 0.5, $P > 0.05$, P values are not corrected) it is denoted by *white*. During wakefulness (W) three parietal channels are significantly lagged in phase, whereas five frontal channels lead in phase relationship. This pattern tends to be disrupted during LOC and returns with the ROC.

8–13 Hz during the waking state is consistent with Stam and van Straaten's modeling study as well as Nolte *et al.*'s[39] experimental result.

The altered phase relationship is associated with the altered primary locations of the hub nodes in the frontal and parietal regions. The strengths of hub structure in the frontal and parietal regions are presented with betweenness centrality of the regions in figure 7C. In particular, the temporal pattern of phase lead–lag relationship of the α band (8–13 Hz) is associated with the switch of dominance of betweenness centrality between frontal and parietal regions (fig. 7C).

Figure 7D represents the directed connections among 21 channels measured by the dPLI for the α frequency band (8–13 Hz). For a certain node i, if average $dPLI_i$ is less than 0.5 (phase lagging against all the other channels) and statistically consistent over all subjects (Wilcoxon signed-rank test with median 0.5, $P < 0.05$), the node i is denoted in black. If average $dPLI_i$ is larger than 0.5 (phase leading against all the other channels) and statistically consistent in the same way, then the node i is denoted in gray. Otherwise, if the $dPLI_i$ is not significant over the subjects, it is denoted in white. During wakefulness and ROC, the channels that lead the other channels in phase are mainly distributed in the frontal regions, whereas the channels that lagged the other channels in phase are mainly distributed in the parietal regions. Additionally, the dPLI between parietal hubs and frontal channels shows high correlation with betweenness centrality of parietal hubs (Pearson correlation, $R = 0.7225$). This finding suggests that the disrupted parietal hub structure is a mechanism for the observed reversal of phase lead–lag relationship in the frontal–parietal network.

Discussion

In this study we applied graph theoretical network analysis to multichannel electroencephalogram recordings during propofol-induced unconsciousness. Network properties of different states of consciousness (wakefulness, LOC, and ROC) were quantitatively studied in order to elucidate the effects of propofol on functional brain networks. First, we found that, despite a diverse effect on functional connectivity as measured by PLI, propofol increased average path length, clustering coefficient and modularity. This suggests that the optimal information integration capacity in the brain is inhibited by anesthetics. Second, propofol mainly affects the hub nodes, which have the top ranking in betweenness and degree centralities. The disruption of hub structure primarily occurred in the parietal region for α and β frequency bands. Third, the effects of propofol on hub structure were associated with a reversal of feedback-dominant connectivity in the conscious state.

Network Topology Correlates Better with State of Consciousness Than Connection Strength

The topological property of the network recovered in association with the recovery of consciousness, but the network connection strength (PLI) did not. The network structure and the connection strength showed dissociable anesthetic response patterns in the recovery state, which is consistent with our past findings obtained with different analytic techniques.[8] In most frequency bands, the global synchrony measure (PLI) of the recovery state did not return to the original level of baseline state. However, average path length, the parietal hub structure, and the feedback-dominant phase relationship almost returned to the baseline level in the recovery state. Thus, network topology may be a more accurate index of conscious or anesthetic states as opposed to measures of synchrony.

Propofol Disrupts Efficient Information Transmission in the Brain

Integration of global neural information in the brain is considered important for consciousness;[40] as such, the disruption of integration capacity may induce the LOC. Our results support these hypotheses. The increased average path length, clustering coefficient, and modularity after anesthesia were quantitative expressions of inefficient global information transmission and altered local brain functions. This result is consistent with recent magnetic resonance imaging studies. With isoflurane-anesthetized rats, Liang *et al.*[9] found that the anterior and posterior cortices were segregated, with significant changes of local network properties. A study of propofol in humans also showed that functional brain networks lose the ability to integrate information, perhaps through a disturbance of long-range functional connectivity.[10]

Propofol Disrupts Hub Structure in the Parietal Region

Together with the impairment of efficient network structure of the waking state, propofol disrupted the hub structure in the parietal region. The dense hub structures, members of the so-called "rich club," in the parietal region play a core role in information integration and transmission in the brain.[26] Precuneus and superior parietal cortex have been reported as strong parietal hubs,[41–44] and deactivation of these regions was observed during propofol- and sevoflurane-induced anesthesia.[45] Our previous study of electroencephalogram networks using different analytic techniques demonstrated a more pronounced effect of propofol on the parietal compared with frontal networks.[8] Hudetz[23] suggested that the disruption of information integration in a network of the posterior parietal cortex is an agent-invariant final common pathway to unconsciousness. This has been supported by recent findings of nitrous oxide in comparison with propofol.[46]

In this study, we also found that, although the parietal hubs are significantly reduced by propofol, the disparity among the nodes in terms of betweenness centrality still remains during the LOC (fig. 4). It is also notable that the hub structure was not completely destroyed after LOC. Instead, the frontal hubs replaced the role of the parietal hubs, which dominate in the waking state. Thus, despite the reduced capacity of information transmission, the global hub structure of the brain network was preserved. This shifting of dominant distribution of hub nodes from parietal to frontal may accompany local network changes. However, it appears that the brain tends to preserve small worldness of networks through a reconfiguration process. This adaptive reconfiguration during anesthesia has been reported in several studies,[7,9,10] in which functional brain networks appeared to preserve the balance between global integration and local segregation (small worldness) by reconfiguring the local topological structure. The reconfiguration of hub structures in the current study shows how small worldness can be maintained, despite significant anesthetic effects on network topology.

The Reversal of Parietal–Frontal Hub Dominance Disrupts Feedback Connectivity

The disruption of the parietal hub structure inhibits the feedback-dominant information flow associated with the conscious state. In a recent simulation study using dPLI, Stam and van Straaten[25] demonstrated that a characteristic posterior hub structure in the brain naturally causes phase lag of posterior activities (hub nodes) with respect to phases of other brain regions (periphery nodes). This is consistent with a flow of information to the posterior parietal hub. As an example of topology defining the direction of information flow, the phase of the core node in a simple star structure lags with respect to the phases of periphery nodes.[25] Based on this simulation result, we hypothesized that the disruption of parietal hub structure may result in

the disruption of the feedback-dominant information flow from frontal to parietal region. In the current study, most hubs (defined by betweenness and degree centrality) in the conscious state were in the parietal region, especially in the α and β frequency bands. The proportion of parietal hubs was clearly diminished after anesthesia and returned with the recovery of consciousness. Regarding the phase lead–lag relationship, dPLI (in particular, of the α band) revealed that the frontal channels lead the parietal channels in the waking state, and then are neutralized after LOC point. This is consistent with the previous simulation study and empirical data studies, which also identified prominence of the α bandwidth in feedback information flow. The preferential inhibition of feedback connectivity from the frontal to parietal region was observed during general anesthesia with different anesthetics such as sevoflurane in humans,[22] propofol in humans,[22,24,37] ketamine in humans,[47] and isoflurane in rats.[48] The current study demonstrates that the phase lag and lead relationship between frontal and parietal regions is associated with the shifting distribution of prominent hub nodes. This suggests an essential role of topological structure for regional phase relationships in the brain. The role of the α band frequency in the phase lead–lag relationship between frontal and parietal regions is notable. Past studies suggest that propofol induces a hypersynchrony of α between the frontal cortex and thalamus,[49] which may interrupt flexible corticortical communication.[50]

Limitations of the Study

This study has a number of limitations. First, a common reference (A2) was used for the connectivity analysis. A common reference is vulnerable to volume conduction, which can produce a bias in connectivity results. Although PLI itself is known as a relatively robust measure with respect to volume conduction, the results still require careful interpretation.[51] The common reference tends to exaggerate spatially coherent and large-scale activity, ignoring changes within small-scale activities. This can be problematic because some studies have reported that anesthetic-induced unconsciousness is related to a decrease of small-scale connectivity.[9,46] Although a Laplacian reference would improve the problem,[46] unevenly distributed channels in our data (mostly in frontal and parietal regions) limited various tests for the effect. Surface Laplacian or source-based analysis with high-resolution electroencephalogram recordings would be highly recommended for future study. Second, because the wave length of β waves (13–25 Hz, approximately 40–60 ms) is comparable to the conduction delay in the brain (<40 ms for long-range connection), there is a potential problem that phase lead–lag relationships can be incorrectly estimated.[25] Thus, we excluded higher-frequency bands (>13 Hz) for the dPLI analysis. Third, the connectivity analysis seems to depend on the type of connectivity measure. For instance, Granger causality produced opposite connectivity results during waking state, showing dominant feedforward connectivity from parietal to frontal region.[52] However, in our study, the dominant feedback connectivity is consistent with the network simulation by Stam and van Straaten.[25] Further studies are warranted. Finally, we did not use target-controlled infusions that modeled effect-site concentrations, but rather a clinically routine bolus dose of propofol. This creates a potential problem because, despite LOC, the cortical dynamics after induction and before recovery may be quite different[53] although we combined them for the purposes of this study (2 min from each). However, we computed network properties using 4-min data in the middle of LOC state and there was no qualitative difference.

Conclusion

Propofol-induced unconsciousness is associated with a reorganization of dominant hubs from the parietal to the frontal region. These results explain the previous observations of preserved small-world organization despite anesthetic-mediated network disruptions. Additionally, the efficiency of information transmission is reduced and the modularity of brain function is enhanced. Finally, the change of network topology (removing the "sinks" in the parietal region) provides a mechanism for the observed selective inhibition of feedback connectivity in association with anesthetic-induced unconsciousness.

References

1. Boveroux P, Vanhaudenhuyse A, Bruno MA, Noirhomme Q, Lauwick S, Luxen A, Degueldre C, Plenevaux A, Schnakers C, Phillips C, Brichant JF, Bonhomme V, Maquet P, Greicius MD, Laureys S, Boly M: Breakdown of within- and between-network resting state functional magnetic resonance imaging connectivity during propofol-induced loss of consciousness. Anesthesiology 2010; 113:1038–53
2. Schrouff J, Perlbarg V, Boly M, Marrelec G, Boveroux P, Vanhaudenhuyse A, Bruno MA, Laureys S, Phillips C, Pélégrini-Issac M, Maquet P, Benali H: Brain functional integration decreases during propofol-induced loss of consciousness. Neuroimage 2011; 57:198–205
3. Martuzzi R, Ramani R, Qiu M, Rajeevan N, Constable RT: Functional connectivity and alterations in baseline brain state in humans. Neuroimage 2010; 49:823–34
4. Stamatakis EA, Adapa RM, Absalom AR, Menon DK: Changes in resting neural connectivity during propofol sedation. PLoS One 2010; 5:e14224
5. Mhuircheartaigh RN, Rosenorn-Lanng D, Wise R, Jbabdi S, Rogers R, Tracey I: Cortical and subcortical connectivity changes during decreasing levels of consciousness in humans: A functional magnetic resonance imaging study using propofol. J Neurosci 2010; 30:9095–102
6. Alkire MT: Loss of effective connectivity during general anesthesia. Int Anesthesiol Clin 2008; 46:55–73
7. Lee U, Oh G, Kim S, Noh G, Choi B, Mashour GA: Brain networks maintain a scale-free organization across consciousness, anesthesia, and recovery: Evidence for adaptive reconfiguration. Anesthesiology 2010; 113:1081–91

8. Lee U, Müller M, Noh GJ, Choi B, Mashour GA: Dissociable network properties of anesthetic state transitions. Anesthesiology 2011; 114:872–81
9. Liang Z, King J, Zhang N: Intrinsic organization of the anesthetized brain. J Neurosci 2012; 32:10183–91
10. Schröter MS, Spoormaker VI, Schorer A, Wohlschläger A, Czisch M, Kochs EF, Zimmer C, Hemmer B, Schneider G, Jordan D, Ilg R: Spatiotemporal reconfiguration of large-scale brain functional networks during propofol-induced loss of consciousness. J Neurosci 2012; 32:12832–40
11. Stephan KE, Hilgetag CC, Burns GA, O'Neill MA, Young MP, Kötter R: Computational analysis of functional connectivity between areas of primate cerebral cortex. Philos Trans R Soc Lond B Biol Sci 2000; 355:111–26
12. Eguíluz VM, Chialvo DR, Cecchi GA, Baliki M, Apkarian AV: Scale-free brain functional networks. Phys Rev Lett 2005; 94:018102
13. Stam CJ: Functional connectivity patterns of human magnetoencephalographic recordings: A 'small-world' network? Neurosci Lett 2004; 355:25–8
14. Bullmore E, Sporns O: The economy of brain network organization. Nat Rev Neurosci 2012; 13:336–49
15. Bassett DS, Bullmore E: Small-world brain networks. Neuroscientist 2006; 12:512–23
16. Bassett DS, Bullmore ET: Human brain networks in health and disease. Curr Opin Neurol 2009; 22:340–7
17. Stam CJ, de Haan W, Daffertshofer A, Jones BF, Manshanden I, van Cappellen van Walsum AM, Montez T, Verbunt JP, de Munck JC, van Dijk BW, Berendse HW, Scheltens P: Graph theoretical analysis of magnetoencephalographic functional connectivity in Alzheimer's disease. Brain 2009; 132(Pt 1):213–24
18. Rubinov M, Knock SA, Stam CJ, Micheloyannis S, Harris AW, Williams LM, Breakspear M: Small-world properties of nonlinear brain activity in schizophrenia. Hum Brain Mapp 2009; 30:403–16
19. Leistedt SJ, Coumans N, Dumont M, Lanquart JP, Stam CJ, Linkowski P: Altered sleep brain functional connectivity in acutely depressed patients. Hum Brain Mapp 2009; 30:2207–19
20. Ponten SC, Bartolomei F, Stam CJ: Small-world networks and epilepsy: Graph theoretical analysis of intracerebrally recorded mesial temporal lobe seizures. Clin Neurophysiol 2007; 118:918–27
21. Lewis LD, Weiner VS, Mukamel EA, Donoghue JA, Eskandar EN, Madsen JR, Anderson WS, Hochberg LR, Cash SS, Brown EN, Purdon PL: Rapid fragmentation of neuronal networks at the onset of propofol-induced unconsciousness. Proc Natl Acad Sci U S A 2012; 109:E3377–86
22. Ku SW, Lee U, Noh GJ, Jun IG, Mashour GA: Preferential inhibition of frontal-to-parietal feedback connectivity is a neurophysiologic correlate of general anesthesia in surgical patients. PLoS One 2011; 6:e25155
23. Hudetz AG: Cortical disintegration mechanism of anesthetic-induced unconsciousness, Suppressing the Mind: Anesthetic Modulation of Memory and Consciousness Mind, 1st edition. Edited by Hudetz AG, Pearce R. Humana Press, New York: 2010, pp 99–125
24. Lee U, Kim S, Noh GJ, Choi BM, Hwang E, Mashour GA: The directionality and functional organization of frontoparietal connectivity during consciousness and anesthesia in humans. Conscious Cogn 2009; 18:1069–78
25. Stam CJ, van Straaten EC: Go with the flow: Use of a directed phase lag index (dPLI) to characterize patterns of phase relations in a large-scale model of brain dynamics. Neuroimage 2012; 62:1415–28
26. van den Heuvel MP, Kahn RS, Goñi J, Sporns O: High-cost, high-capacity backbone for global brain communication. Proc Natl Acad Sci U S A 2012; 109:11372–7
27. Stam CJ, Nolte G, Daffertshofer A: Phase lag index: Assessment of functional connectivity from multi channel EEG and MEG with diminished bias from common sources. Hum Brain Mapp 2007; 28:1178–93
28. Schreiber T, Schmitz A: Surrogate time series. Physica D 2000; 142:346–82
29. Latora V, Marchiori M: Efficient behavior of small-world networks. Phys Rev Lett 2001; 87:198701
30. Watts DJ, Strogatz SH: Collective dynamics of 'small-world' networks. Nature 1998; 393:440–2
31. Onnela JP, Saramäki J, Kertész J, Kaski K: Intensity and coherence of motifs in weighted complex networks. Phys Rev E Stat Nonlin Soft Matter Phys 2005; 71(6 Pt 2):065103
32. Newman ME: Modularity and community structure in networks. Proc Natl Acad Sci U S A 2006; 103:8577–82
33. Newman ME: Finding community structure in networks using the eigenvectors of matrices. Phys Rev E Stat Nonlin Soft Matter Phys 2006; 74(3 Pt 2):036104
34. Blondel VD, Guillaume JL, Lambiotte R, Lefebvre E: Fast unfolding of communities in large networks. J Stat Mech 2008; 10:10008
35. Rubinov M, Sporns O: Complex network measures of brain connectivity: Uses and interpretations. Neuroimage 2010; 52:1059–69
36. Maslov S, Sneppen K: Specificity and stability in topology of protein networks. Science 2002; 296:910–3
37. Boly M, Moran R, Murphy M, Boveroux P, Bruno MA, Noirhomme Q, Ledoux D, Bonhomme V, Brichant JF, Tononi G, Laureys S, Friston K: Connectivity changes underlying spectral EEG changes during propofol-induced loss of consciousness. J Neurosci 2012; 32:7082–90
38. Boly M, Garrido MI, Gosseries O, Bruno MA, Boveroux P, Schnakers C, Massimini M, Litvak V, Laureys S, Friston K: Preserved feedforward but impaired top-down processes in the vegetative state. Science 2011; 332:858–62
39. Nolte G, Ziehe A, Nikulin VV, Schlögl A, Krämer N, Brismar T, Müller KR: Robustly estimating the flow direction of information in complex physical systems. Phys Rev Lett 2008; 100:234101
40. Tononi G: Consciousness as integrated information: A provisional manifesto. Biol Bull 2008; 215:216–42
41. Gong G, He Y, Concha L, Lebel C, Gross DW, Evans AC, Beaulieu C: Mapping anatomical connectivity patterns of human cerebral cortex using *in vivo* diffusion tensor imaging tractography. Cereb Cortex 2009; 19:524–36
42. Hagmann P, Cammoun L, Gigandet X, Meuli R, Honey CJ, Wedeen VJ, Sporns O: Mapping the structural core of human cerebral cortex. PLoS Biol 2008; 6:e159
43. Achard S, Salvador R, Whitcher B, Suckling J, Bullmore E: A resilient, low-frequency, small-world human brain functional network with highly connected association cortical hubs. J Neurosci 2006; 26:63–72
44. Jäncke L, Langer N: A strong parietal hub in the small-world network of coloured-hearing synaesthetes during resting state EEG. J Neuropsychol 2011; 5:178–202
45. Kaisti KK, Metsähonkala L, Teräs M, Oikonen V, Aalto S, Jääskeläinen S, Hinkka S, Scheinin H: Effects of surgical levels of propofol and sevoflurane anesthesia on cerebral blood flow in healthy subjects studied with positron emission tomography. Anesthesiology 2002; 96:1358–70
46. Kuhlmann L, Foster BL, Liley DT: Modulation of functional EEG networks by the NMDA antagonist nitrous oxide. PLoS One 2013; 8:e56434
47. Lee U, Ku S, Noh G, Baek S, Choi B, Mashour GA: Disruption of frontal-parietal communication by ketamine, propofol, and sevoflurane. Anesthesiology 2013; 118:1264–75
48. Imas OA, Ropella KM, Wood JD, Hudetz AG: Isoflurane disrupts anterio-posterior phase synchronization of

flash-induced field potentials in the rat. Neurosci Lett 2006; 402:216–21

49. Ching S, Cimenser A, Purdon PL, Brown EN, Kopell NJ: Thalamocortical model for a propofol-induced alpha-rhythm associated with loss of consciousness. Proc Natl Acad Sci U S A 2010; 107:22665–70
50. Supp GG, Siegel M, Hipp JF, Engel AK: Cortical hypersynchrony predicts breakdown of sensory processing during loss of consciousness. Curr Biol 2011; 21:1988–93
51. Peraza LR, Asghar AU, Green G, Halliday DM: Volume conduction effects in brain network inference from electroencephalographic recordings using phase lag index. J Neurosci Methods 2012; 207:189–99
52. Barrett AB, Murphy M, Bruno MA, Noirhomme Q, Boly M, Laureys S, Seth AK: Granger causality analysis of steady-state electroencephalographic signals during propofol-induced anaesthesia. PLoS One 2012; 7:e29072
53. Friedman EB, Sun Y, Moore JT, Hung HT, Meng QC, Perera P, Joiner WJ, Thomas SA, Eckenhoff RG, Sehgal A, Kelz MB: A conserved behavioral state barrier impedes transitions between anesthetic-induced unconsciousness and wakefulness: Evidence for neural inertia. PLoS One 2010; 5:e11903